

Chemical pathways in ultracold reactions of SrF molecules

Edmund R. Meyer* and John L. Bohn

JILA, NIST, and Department of Physics, University of Colorado, Boulder, Colorado 80309-0440, USA

(Received 20 December 2010; published 23 March 2011)

We present a theoretical investigation of the chemical reaction $\text{SrF} + \text{SrF} \rightarrow \text{products}$, focusing on reactions at ultralow temperatures. We find that bond swapping $\text{SrF} + \text{SrF} \rightarrow \text{Sr}_2 + \text{F}_2$ is energetically forbidden at these temperatures. Rather, the only energetically allowed reaction is $\text{SrF} + \text{SrF} \rightarrow \text{SrF}_2 + \text{Sr}$, and even then only singlet states of the SrF_2 trimer can form. A calculation along a reduced reaction path demonstrates that this abstraction reaction is barrierless and proceeds by one SrF molecule “handing off” a fluorine atom to the other molecule.

DOI: [10.1103/PhysRevA.83.032714](https://doi.org/10.1103/PhysRevA.83.032714)

PACS number(s): 34.20.Gj, 34.50.Ez, 34.50.Lf

I. INTRODUCTION

After many years of experimental effort, chemical reaction dynamics has now entered the cold and ultracold regimes. Robust techniques such as buffer-gas cooling [1] and Stark deceleration [2] have pushed the energy resolution of molecular beam techniques down to the milli-Kelvin level, resulting in new probes of chemical dynamics [3–6]. Extending the low-energy limit even further, coherent optical techniques have produced samples of alkali-metal dimers in their absolute ground state, at temperatures in the 1- to 100- μK range [7–10]. These ultracold molecules are so exquisitely sensitive to comparatively weak influences that chemistry can be studied and controlled by exploiting quantum statistics [11], electric fields [12], and confinement in optical lattices [13–16].

With these new capabilities naturally come questions of what can be learned about chemical reaction dynamics under these novel circumstances. The *manipulation* of chemical reactions by external electric and magnetic fields relies heavily on the behavior of long-range physics, where the molecules exert, say, dipolar forces on one another, but are too far away from one another to react. Indeed, the theoretical analysis of the reaction $2\text{KRb} \rightarrow \text{K}_2 + \text{Rb}_2$, observed and studied at JILA, took this point of view by treating the actual reaction as a nearly perfectly absorbing “black box,” which removed the molecules when they got close enough together but without regard for what exactly happened to them [17,18].

To *understand* more about chemical dynamics from these experiments would presumably require a scattering simulation on a complete four-body potential energy surface (PES) for the K-K-Rb-Rb system, which does not yet exist. In recent work, however, Byrd *et al.* have described the main salient features of this surface [19]. First, along its main reaction coordinate, the reaction presents no energetic barrier to reaction (consistent with the high-reaction rates observed at JILA). Second, its transition state, at the borderline between reactants and products, represents a T-geometry characteristic of an insertion reaction, wherein a K atom from one molecule inserts itself between the K and Rb of the other. This circumstance suggests that the reaction proceeds with a complicated four-body dance of the involved atoms, which may be revealed at

ultralow temperatures by characterizing the resonant states of the complex. Observing these transition-state resonances and interpreting their influence in chemical reactions is a long-standing goal of physical chemistry and one in which the high-energy resolution of ultracold molecules may be of great help.

Set against this backdrop, it would also be useful to explore other molecules reacting at ultralow temperatures to gain additional insight into what can be learned. To this end, the SrF molecule is an appealing candidate and the one with which we deal with in this article. SrF is a prime example of a class of molecules that have been identified as amenable to direct laser cooling from a beam [20], and in fact laser cooling has been recently demonstrated [21]. It is quite polar (dipole moment ≈ 1.4 D), so that electric field manipulation is a possibility. Moreover, it has an open-shell $^2\Sigma$ ground state that gives it a magnetic moment as well. This circumstance opens opportunities such as trapping the molecules magnetically, while manipulating their interactions electrically [22].

In this article, we explore the possibility and mechanisms for chemical reactions of SrF molecules at ultralow temperatures. We make several observations. First, the exchange reaction



is energetically disallowed, as might be expected for a reaction that turns two ionic bonds into two covalent ones. Therefore, the reaction, if it happens at all, must proceed with an abstraction reaction in which an atom jumps from one molecule to the other. This is exactly the opposite situation from what occurs in KRb, where the exchange is the only possible reaction, and then only just barely [19,23,24].

Second, we find that the Sr-abstraction reaction



cannot occur at low temperature, whereas the F-abstraction reaction



can occur, as it produces the deeply bound SrF_2 trimer. Moreover, this reaction, which is barrierless, can only occur in the singlet channel, that is, only if the reaction takes place on the PES with total electronic spin $S = 0$. Therefore, chemical reactions are expected to occur at quite high rates

*present address: Department of Physics, Kansas State University; meyere@phys.ksu.edu.

for unpolarized SrF molecules, while they should be strongly suppressed for spin-polarized SrF, which scatter primarily on the triplet surface. Spin-rotation couplings will ensure that this suppression is not complete [25]. Nevertheless, one must be mindful of any opportunity to suppress inelastic collisions, as they can easily destabilize the gas and derail attempts to exploit the molecules for many-body physics applications.

Third, we describe the basic physics of the abstraction process by looking at a restricted version of the four-body PES. We find that the F end of one SrF molecule approaches the Sr end of the other, as dictated by the dipole-dipole interaction between molecules. Next, the F atom is handed off from one molecule to the other, and the free Sr goes off by itself. By this handoff mechanism it is possible that the reaction proceeds without forming a resonant complex and that its interpretation from ultracold collision data may be more straightforward than the complete re-arrangement necessary in reactions of KRb. In any event, complementary dynamics should give us complementary insights into these quite different reactions.

II. AB INITIO CALCULATIONS

In this section, we will study the relevant molecular species: the dimers SrF, Sr₂, and F₂ and the trimers SrF₂ and Sr₂F. All calculations of these species are performed using the MOLPRO suite of *ab initio* electronic structure codes [26]. We use the relativistic effective core potential and associated basis set of the Stuttgart group for Sr [27] (ECP28MDF) and the augmented, correlation consistent valence triple (quadruple) ζ basis set [AVTZ (AVQZ)] of Dunning for F [28]. For the diatomic properties, the AVQZ basis is used.

We perform the calculations by first computing a spin-restricted Hartree-Fock (RHF) wave function as a starting guess for a coupled-cluster singles, doubles, and noniterative triples excitation calculation [CCSD(T)] [29]. The minimum energy configuration is obtained using the method of steepest descents. Properties such as dipole moment, polarizability, and quadrupole moment are calculated using the finite-field approach. To compare the energies to the free-atom limit, we use basis set superposition error (BSSE) corrections as given by the method of Boys and Bernardi [30]. We calculate the vibrational frequencies by making the symmetry-independent displacements of the atoms and calculating the Hessian within the MOLPRO suite of routines.

A. Diatomic species

In the collision of two SrF molecules there are three diatomic species to consider: the reactant SrF and the possible products Sr₂ and F₂. In the following, we will investigate the relevant diatomic properties such as equilibrium bond length, well depth, and vibration constant. But first, an exercise in bond strengths can immediately inform us as to whether the reactions in Eq. (1) can occur. On the left-hand side (LHS) of the reaction we have two ionic bonds. On the right-hand side (RHS) we have one van der Waals bond and one covalent bond; the former is very weak and the latter is usually less bound than an ionic bond. An ionic bond can be thought of as a strengthening of the single covalent bond because of a transferring of charge from one atom to the other. From these

simple considerations, we conclude that the reaction in (1) is energetically unfavorable at ultracold temperatures.

Sr₂ is a van der Waals molecule. The ¹S₀ atomic structure means that the the outer *s* electrons are already paired up and therefore play a limited role in the bonding of two Sr atoms. Previous work has shown that this molecule is not deeply bound, with a well depth of $D_e = 1081.8 \text{ cm}^{-1}$ [31,32]. Because of the large binding length and relatively larger mass of Sr atoms, the vibrational constant is fairly small, $\omega_e = 40.3 \text{ cm}^{-1}$ [32]. Therefore, the energy required to dissociate this molecule from the zeroth vibrational level is given by $D_0 = 1061.6 \text{ cm}^{-1}$.

F₂ is a covalently bonded species, with a ground state of ¹ Σ_g^+ symmetry. F₂ has an appreciably large binding energy of $D_0 = 12\,950 \text{ cm}^{-1}$ [33] and much smaller bond length than Sr₂. The unpaired *p* electrons in the F atoms pair up and form a fairly deep well. Because of the lighter mass and tighter confining potential, the F₂ molecule has a comparatively large vibrational constant, 917 cm^{-1} [34]. Therefore, the well depth $D_e = 13\,410 \text{ cm}^{-1}$ when combining the work of Refs. [33] and [34].

SrF is a highly polar molecule. The willingness of F to take an extra electron, and of Sr to give one up, would lead one to conclude that at the minimum of the well the molecule is well described by a Sr⁺F⁻ configuration. We therefore compared the optimized geometry calculated at the RHF-CCSD(T)+BSSE calculation in two ways. The first was to compare the energy at the bottom of the potential energy surface to that of free Sr and F atoms. The other was to compare to free Sr⁺ and F⁻ ions and then calculate the ionization potential of Sr and the electron affinity of F. These calculations agreed with each other to within several centimeters⁻¹. The well depth D_e we report here refers to the energy difference between the individually separated neutral atoms Sr and F and the bottom of the potential well of SrF.

In Table I, we present the results of our RHF-CCSD(T)+BSSE calculations. All bond lengths (R_e) are in angstroms (Å), well depths (D_e) and vibration constants (ω_e) are in centimeters⁻¹, and associated dipole and quadrupole

TABLE I. The molecular properties of Sr₂, F₂, and SrF. Energies are in centimeters⁻¹, bond lengths are in angstroms, and moments are in atomic units. Experimental values are given where known.

Molecule	D_e	R_e	ω_e	d_m	α_z	θ_{zz}
SrF (this work)	44 200	2.084	499	1.38	126	8.95
Expt.	45 290 (560) ^a	2.075 ^b	502.4 ^b	1.36 ^c		
Theory	45 000 ^d	2.085	507			
Sr ₂ (this work)	820	4.773	36.2			
Expt. ^e	1081.8	4.672	40.3			
F ₂ (this work)	12 880	1.410	927			
Expt.	13 410 ^f	1.411 ^g	917 ^g			

^aReference [35].

^bReference [36].

^cReference [37].

^dReference [38].

^eReference [32].

^fReference [33], ZEKE and ion-pair imaging D_0 adjusted by ω_e of Ref. [34].

^gReference [34].

moments (d_m and θ_{zz}) are in atomic units (ea_0 and ea_0^2 , respectively). The corresponding experimental values are from the references given, and uncertainties are printed for those where the value was reported. The theoretical calculation of Langhoff *et al.* is done at the configuration interaction with single- and double-excitation levels of theory [38]. Our current method yields a well depth smaller than the experimentally obtained value by 2σ [35]. The bond length is in good agreement with that of Ref. [38]. From these results, we immediately see that the reaction in Eq. (1) is energetically forbidden, by more than $70\,000\text{ cm}^{-1}$, and is of no concern in an ultracold gas.

B. Triatomic species

There are two different triatomic species to consider as given in Eqs. (2) and (3). At first glance, we might think both are quite easily allowed. From a simple bond-strength argument, we can see that one is favored over the other. In particular, the triatom in Eq. (2) is less bound than the triatom in Eq. (3). The triatom in (3) has two ionic bonds, while the triatom in (2) can have only one. Therefore, from the fact that two ionic bonds should be more deeply bound than one, we expect the triatom in (3) to be more deeply bound than that in (2). In addition, it is expected that the reaction in (2) is energetically unfavorable because there are stronger bonds on the LHS than on the RHS. However, the reaction in (3) cannot be determined from these arguments. Thus, it is to be calculated using the same *ab initio* methods as in the previous section. For the SrF_2 singlet state, we use the AVQZ basis for F as we did for SrF . However, for the remaining states we only used the AVTZ basis. This is because these states are so energetically forbidden (as we will see) that the less time-consuming calculation is adequate for our purposes.

In Fig. 1, we give the three coordinates that are used in the optimization of the geometry. Using these three coordinates (r_1 , r_2 , and θ), without constraining them, ensures that the electronic wave function belongs to the C_s symmetry group. Thus, there are electronic states with even (A') and odd (A'') reflection symmetries through the plane containing the three atoms. When the two bond lengths are equal, the symmetry group is instead expanded to C_{2v} . This added symmetry describes whether the molecule possesses even or odd reflections about the line which bisects the homonuclear bond. Where the ground state has equal bond lengths, we

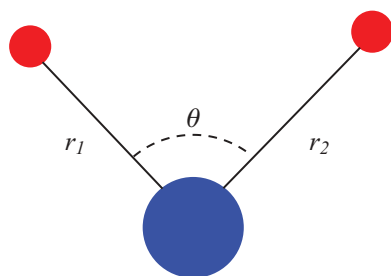


FIG. 1. (Color online) Diagram of the geometries considered in the calculation of the molecules Sr_2F and SrF_2 . The coordinates r_1 , r_2 , and θ were varied and energy optimized to find the minimum energy configuration in both the A' and A'' symmetry groups.

TABLE II. The molecular properties of SrF_2 and Sr_2F . Energies are in cm^{-1} , bond lengths are in angstroms, and angles are in degrees. Previous theoretical values are given where applicable.

Molecule	Symmetry	D_e	r_1	r_2	θ
SrF_2	1A_1	91 870	2.13	2.13	135.7
Theory ^a			2.16	2.16	138.8
Expt. ^b		89 300 to 91 900			
Sr_2F	2B_2	52 300	2.26	2.26	115.8
Sr_2F	2B_1	43 900	2.25	2.25	101.7
SrF_2	$^3A''$	43 400	2.10	3.72	70.4

^aReference [39].

^bReference [40]. Extracted from enthalpy of formation.

have indicated this with the appropriate notation; A_1 (B_2) have even (odd) reflection symmetry about the midpoint between the homonuclear bond and even reflection symmetry through the plane containing the three atoms. Similarly, A_2 (B_1) has odd (even) reflection about the midpoint of the homonuclear bond with odd reflection through the plane containing the three atoms.

In Table II, we present the results of the RHF-CCSD(T)+BSSE calculation. As is evident, the most deeply bound trimer is given by the 1A_1 symmetry for SrF_2 . It is also the only one for which previous theoretical work is available for comparison. In Ref. [39], Kaupp *et al.* presented a theoretical study of many alkaline-earth metal atoms with two halogen atoms. We note that alkaline-earth dihalides have historically been of significant interest in chemistry, as some have bent geometries (and hence possess permanent dipole moments in their body frame) and some are linear (with no such dipole moment). A bend is not expected from classical models of charged particles interacting, and therefore correctly predicting the bend is a measure of the quality of the wave function. This is because the bend is a result of the presence of d -electron orbitals on the ground state. Our calculation agrees well with that of Ref. [39] in the description of the bond length and bending angle. We present the energy required to pull apart the molecule into its atomic constituents, atomization. This energy is greater than that of two SrF molecules and therefore, in the absence of a barrier, should react chemically at ultracold temperatures.

The triplet SrF_2 molecule (last line of Table II) is far less bound, and indeed has binding energy similar to that of a single SrF molecule. A simple way to understand this is to think of this as a triplet covalent bond in F_2 with a Sr atom bound ionically to one or the other F atoms. The triplet bond in F_2 is much shallower than the singlet covalent bond in the ground state. Then the Sr comes along and binds to one of the F atoms. A simple charge population analysis shows that only the F atom closer to Sr captures charge. Importantly, the triplet trimer is energetically disallowed at ultracold-temperature (and even room-temperature) SrF collisions.

The other potential trimer, Sr_2F , is reported in the second and third lines of Table II. This molecule, while more deeply bound than the triplet state of SrF_2 , is not deep enough to be chemically reactive, as expected from the simple bond arguments. Thus, this reaction will not proceed at ultracold temperatures. Notice that this molecule has a binding energy

only slightly more than that of a single SrF diatom. The doublet nature of this molecule is due to the one unpaired electron that can be viewed as coming from the F atom plus a Sr₂ bond or from the doublet nature of SrF plus a free Sr atom.

We therefore conclude that only the singlet electronic state of SrF₂ will form in the collision of two SrF molecules at ultralow collision energy. We find that the energy released is 3470 cm⁻¹. To be thorough, we must take into account the zero-point vibrational energy of the systems in consideration. In Table I, we gave the calculated and experimental values of the vibrational constants of SrF. We have calculated the vibrational constants of SrF₂ in the singlet electronic state: $\omega_{\text{sym}} = 472.9$, $\omega_{\text{asym}} = 478.7$, and $\omega_{\text{bend}} = 79.3$ cm⁻¹, where these represent the symmetric (or breathing) mode, the antisymmetric mode, and the bending mode of the triatomic molecule. This yields a zero-point energy of 515.5 cm⁻¹. Therefore, all the exoergic reactions are reduced by ≈ 20 cm⁻¹. It is evident that the added vibrational modes (three vs one in the diatom SrF) are not enough to overcome the energy released in the chemical reaction. In fact, there are roughly 150 vibrational states accessible in the reactants, using the calculated exoergic of $\Delta_{\text{trimer}} = 3450$ cm⁻¹.

To our knowledge, this quantity has been measured only once, in a gas cell which maintained chemical equilibrium between reactants and products at ~ 1500 K, using mass spectroscopy to measure their relative abundance [41]. Knowing the temperature, this measurement provided information on the enthalpy of formation $\Delta_f H$, which corresponds to the energy released ΔE_{trimer} in Eq. (3). This measurement agrees that the reaction is exothermic, but by a more modest value of $\Delta_f H = 2.1$ kcal/mol = 740 cm⁻¹ than we have calculated. Given that the experimental uncertainty was comparable to 700 cm⁻¹ and our computational uncertainty is perhaps 2000 cm⁻¹, the results are not too seriously in disagreement. Ultimately, measurements in laser-cooled SrF samples should sort out this issue in detail.

III. REACTION PATH BASICS

To compute the full PES of the four-body system involved in the reaction is of course a complicated affair. Here, we instead compute selected slices of this PES. One is a reaction-path coordinate version that will verify that the reaction is barrierless. The second is a more detailed examination of the handoff mechanism that drives this abstraction reaction. We will focus exclusively on the singlet PES, as it is the only one leading to reactions in an ultralow temperature SrF gas. All calculations are performed with the ECP28MDF basis set and ECP of the Stuttgart group for Sr along with the AVTZ basis of Dunning for F. We use the RHF-CCSD(T)+BSSE level of theory.

A basic idea in constructing the reaction path surface is that the relatively heavy Sr atoms move comparatively slowly, and therefore the Sr-Sr distance can be regarded (approximately) as an adiabatic coordinate. Fixing this distance, denoted $R_{\text{Sr-Sr}}$, we optimize the coordinates r_1 , r_2 , θ_1 , and θ_2 of the F atoms, as defined in Fig. 2, so as to minimize the energy. For simplicity, we constrain all four atoms to lie in a plane. While this limits the possibility of the molecules changing the dihedral angle, it does not prevent all insertion-type configurations from

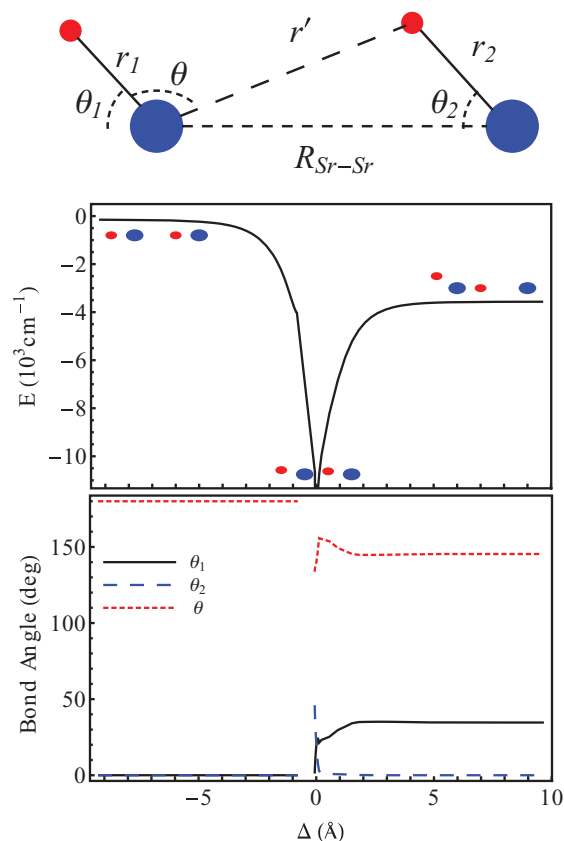


FIG. 2. (Color online) The top portion of the figure describes the geometry of the situation; r_1 , r_2 , θ_1 , and θ_2 are optimized so as to produce the minimal energy for a fixed $R_{\text{Sr-Sr}}$. The LHS describes the approach of two dipole objects. On the RHS, the approach is more van der Waals-like where the polar SrF₂ polarizes the Sr atom. The middle is a sharp point that is an artifact of the choice of $\Delta = r_2 - r'$. The larger, blue (smaller, red) filled disks represent Sr (F) atoms. The approach to the transition state near $\Delta = 0$ Å is very nearly linear up to the point of F capture. Then θ_1 and θ_2 rotate to form a complex which contains a slightly distorted SrF₂ configuration. The lowest panel shows the optimized angles θ_1 (solid, black line), θ_2 (large dashed, blue line), and θ (small dashed, red line). The values remain fairly constant for $|\Delta| > 1$ Å and change to form the transition state in the region $|\Delta| < 1$ Å.

being explored. As we will see, the optimizations of the other coordinates suggest a preference for linear orientations upon approach.

To track the progress of the reaction, we define the approximate reaction coordinate Δ via

$$\Delta = r_2 - r'. \quad (4)$$

In the limit that Δ is negative and large, it denotes the distance between the two SrF diatoms, whereas when Δ is positive and large, it refers to the distance between the SrF₂ trimer and the free Sr atom.

The optimized energy is plotted as a function of Δ in the middle panel of Fig. 2, adjusted so that the zero energy refers to two free, separated SrF molecules. The PES along this path shows very little structure: it corresponds to almost pure dipolar attraction between reactants for $\Delta < 0$ and almost pure van der Waals attraction between the products for $\Delta > 0$.

In particular, this cut through the PES shows clearly that there is *no barrier* to reaction, at least along the minimum-energy path.

This choice of reaction coordinate is useful, but it also leads to a structural discontinuity in the surface of Fig. 2. This discontinuity is made clear in the last panel of Fig. 2, which depicts the variation in the angles θ_1 , θ_2 , and θ (see top panel of Fig. 2). This is an artifact of the choice in approximate reaction coordinate. Physically, this discontinuity arises because $R_{\text{Sr-Sr}}$ is not strictly an adiabatic coordinate. At some point, the intermediate F atom glides from its local minimum (attached to the right-hand Sr atom) to its global minimum (attached to the SrF on the left). When this occurs, a single value of $R_{\text{Sr-Sr}}$ corresponds to two distinct values of the reaction coordinate Δ where the adiabatic energy is the same. This mechanism will be clarified by looking at the PES from a different perspective.

For $\Delta < 0$, the system is described by a linear geometry ($\theta_1 = \theta_2 = 0^\circ$). As the diatoms approach one another, they reach a location in Δ where the discontinuity occurs. From the $\Delta > 0$ side, the values of θ_1 , θ_2 , and θ are fairly constant. As Δ is decreased toward zero by decreasing $R_{\text{Sr-Sr}}$, the four-atom system reaches a minimum near $\Delta = 0$. As the $R_{\text{Sr-Sr}}$ is decreased further, θ_1 approaches 0° and the system approaches the geometrical discontinuity from the other side. This leads to a fairly smooth reaction path in the coordinate Δ but hides the change in the geometrical configuration of the four-atom system.

Using the information contained in the values of θ_1 , θ_2 , and θ , we are led to study the F capture process by analyzing the linear configuration. Even though the final trimer's ground state is bent, the energy of the linear configuration is only $\sim 500 \text{ cm}^{-1}$ above the bent configuration of SrF_2 . For this reason, we can make a reasonable qualitative description of the reaction by constraining all atoms to lie on a line, as in the upper panel of Fig. 3.

We again treat the Sr-Sr distance as an adiabatic coordinate. Then, for fixed Sr-Sr distances $R_{\text{Sr-Sr}}$, we vary the location of the middle F atom, describing it with coordinate r' as depicted at the top of Fig. 3. The leftmost F atom is fixed to the diatom bond length of SrF, r_1 . Because the bond lengths in SrF and SrF_2 are so similar, this is a reasonable assumption. Using the RHF-CCSD(T)+BSSE method, we calculate the potential experienced by the middle F atom. The results are presented in Fig. 3 for various values of $R_{\text{Sr-Sr}}$. The BSSE compares the energy to the atomization limit. In the figure, we offset the energy by the binding energy of two SrF molecules. Thus, zero energy is the energy of two SrF diatoms.

In the first plot of Fig. 3, the two Sr atoms are far from one another. The potential for the F atom has two minima, representing the fluorine attached to the original Sr atom (right-hand well) or else attached to the other SrF to form the product SrF_2 (left-hand well). The latter well being deeper signifies that the products $\text{SrF}_2 + \text{Sr}$ are energetically favored and the reaction is exoergic, even within a strictly linear geometry. Between these minima stands a high barrier, which naturally prevents the F atoms from jumping from reactants to products when the Sr atoms are this far apart.

In subsequent panels of Fig. 3, the two Sr atoms approach one another. In each case, the barrier lowers until it eventually disappears altogether, and the F atom rests at the bottom of a

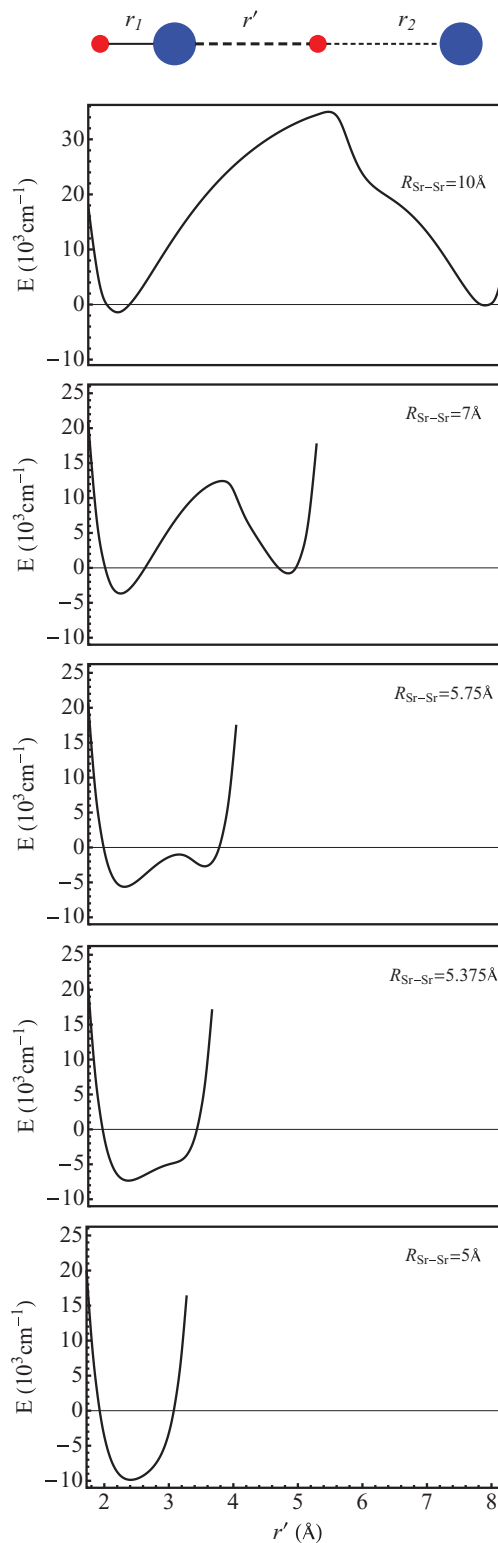


FIG. 3. (Color online) The top portion gives the geometry of the system. The bond length r_1 is fixed while r_2 is varied; r' gives the distance of the middle F to the other Sr atom and is called the handoff coordinate since it describes the handing off of a F to one Sr from the other Sr. Each subsequent plot is for a fixed value of $R_{\text{Sr-Sr}}$ given in the upper RHS. As the value of $R_{\text{Sr-Sr}}$ is reduced, the barrier to forming the system $\text{F-Sr-F} + \text{Sr}$ is diminished until it no longer stops the transfer of F. The calculations were performed at the RHF-CCSD(T) + BSSE with the Sr ECP28MDF and F AVTZ bases, respectively.

single minimum in the last plot of Fig. 3. This configuration defines the four-body transition state with $\Delta \approx 0 \text{ \AA}$. At this point the Sr atom can recede, and to the extent that its motion really is adiabatic, the F atom will tend to remain in the lower well, thus finding itself a part of the SrF₂ final product. We say that this F-abstraction reaction occurs by a handoff mechanism, whereby the right-hand Sr atom approaches, gently hands off the F, and then goes away. As compared to the KRb-KRb surface [19], this reaction is less likely to partake in a complicated dance of the four atoms, becoming thoroughly enmeshed in a four-body transition-state complex.

IV. CONCLUSIONS

In summary, we have established that ground-state SrF molecules will indeed be chemically reactive, even at ultralow temperatures that will be achieved via laser cooling. The only possible outcome of such a reactive collision would be the singlet trimer SrF₂, plus a free Sr atom. Because of

the need to produce a singlet final state, chemical reactivity should be strongly suppressed in a spin-polarized sample. This species therefore looks like a promising candidate for ultracold molecular studies. On the one hand, SrF may serve as a useful platform for probing and understanding abstraction reactions in unprecedented detail. On the other hand, if producing a spin-polarized sample suppresses reactions sufficiently, there is also hope that the molecules may live long enough to perform interesting experiments on dipolar degenerate quantum gases. To estimate if this is so, future work will need to study in more detail both the triplet surface and its detailed coupling to the reactive singlet surface.

ACKNOWLEDGMENTS

We are grateful for support from the NSF. We acknowledge useful discussions with G. Quémener about chemical reaction processes.

-
- [1] W. Campbell and J. Doyle, in *Cold Molecules: Theory, Experiment, and Applications*, edited by R. V. Krems, W. C. Stwalley, and B. Friedrich (CRC Press, Boca Raton, FL, 2009), p. 473.
- [2] S. Y. T. van der Meerakker, H. L. Bethlem, and G. Meijer, in *Cold Molecules: Theory, Experiment, and Applications*, edited by R. V. Krems, W. C. Stwalley, and B. Friedrich (CRC Press, Boca Raton, FL, 2009), p. 509.
- [3] L. Scharfenberg, J. Klos, P. J. Dagdigian, M. H. Alexander, G. Meijer, and S. Y. T. van der Meerakker, *Phys. Chem. Chem. Phys.* **12**, 10660 (2010).
- [4] M. Hummon, T. Tscherbül, J. Klos, H. I. Lu, E. Tsikata, W. Campbell, A. Dalgarno, and J. M. Doyle, e-print [arXiv:1009.2513](https://arxiv.org/abs/1009.2513).
- [5] B. C. Sawyer, B. K. Stuhl, M. Yeo, T. V. Tscherbül, M. T. Hummon, Y. Xia, J. Klos, D. Patterson, J. M. Doyle, and J. Ye, e-print [arXiv:1008.5127v1](https://arxiv.org/abs/1008.5127v1).
- [6] L. P. Parazzoli, N. J. Fitch, P. S. Zuchowski, J. M. Hutson, and H. J. Lewandowski, e-print [arXiv:1101.2886](https://arxiv.org/abs/1101.2886) (2011).
- [7] J. M. Sage, S. Sainis, T. Bergeman, and D. DeMille, *Phys. Rev. Lett.* **94**, 203001 (2005).
- [8] K.-K. Ni, S. Ospelkaus, M. Miranda, A. Peer, B. Neyenhuis, J. Zirbel, S. Kotochigova, P. Julienne, D. Jin, and J. Ye, *Science* **322**, 231 (2008).
- [9] J. G. Danzl, M. J. Mark, E. Haller, M. Gustavvson, R. Hart, J. Aldegunde, J. M. Hutson, and H.-C. Nägerl, *Nature Phys.* **6**, 265 (2010).
- [10] K. Aikawa, D. Akamatsu, M. Hayashi, K. Oasa, J. Kobayashi, P. Naidon, T. Kishimoto, M. Ueda, and S. Inouye, *Phys. Rev. Lett.* **105**, 203001 (2010).
- [11] S. Ospelkaus, K.-K. Ni, D. Wang, M. H. G. de Miranda, B. Neyenhuis, G. Quémener, P. S. Julienne, J. L. Bohn, D. S. Jin, and J. Ye, *Science* **327**, 853 (2010).
- [12] K.-K. Ni, S. Ospelkaus, D. Wang, G. Quémener, B. Neyenhuis, M. H. G. de Miranda, J. L. Bohn, J. Ye, and D. S. Jin, *Nature (London)* **464**, 1324 (2010).
- [13] A. V. Gorshkov, P. Rabl, G. Pupillo, A. Micheli, P. Zoller, M. D. Lukin, and H. P. Buchler, *Phys. Rev. Lett.* **101**, 073201 (2008).
- [14] G. Quémener and J. L. Bohn, *Phys. Rev. A* **83**, 012705 (2011).
- [15] A. Micheli, Z. Idziaszek, G. Pupillo, M. A. Baranov, P. Zoller, and P. S. Julienne, *Phys. Rev. Lett.* **105**, 073202 (2010).
- [16] M. H. G. de Miranda, A. Chotia, B. Neyenhuis, D. Wang, G. Quémener, S. Ospelkaus, J. L. Bohn, J. Ye, and D. S. Jin, [arXiv:1010.3731v1](https://arxiv.org/abs/1010.3731v1).
- [17] Z. Idziaszek, G. Q. Quémener, J. L. Bohn, and P. S. Julienne, *Phys. Rev. A* **82**, 020703 (2010).
- [18] Z. Idziaszek and P. S. Julienne, *Phys. Rev. Lett.* **104**, 113202 (2010).
- [19] J. N. Byrd, J. J. A. Montgomery, and R. Côté, *Phys. Rev. A* **82**, 010502 (2010).
- [20] E. S. Shuman, J. F. Barry, D. R. Glenn, and D. DeMille, *Phys. Rev. Lett.* **103**, 223001 (2009).
- [21] E. S. Shuman, J. F. Barry, and D. DeMille, *Nature* **467**, 820 (2010).
- [22] B. C. Sawyer, B. L. Lev, E. R. Hudson, B. K. Stuhl, M. Lara, J. L. Bohn, and J. Ye, *Phys. Rev. Lett.* **98**, 253002 (2007).
- [23] P. S. Zuchowski and J. M. Hutson, *Phys. Rev. A* **81**, 060703 (2010).
- [24] E. R. Meyer and J. L. Bohn, *Phys. Rev. A* **82**, 042707 (2010).
- [25] T. V. Tscherbül, J. Klos, L. Rajchel, and R. V. Krems, *Phys. Rev. A* **75**, 033416 (2007).
- [26] H.-J. Werner *et al.*, MOLPRO, version 2008.3, a package of *ab initio* programs (2008); see <http://www.molpro.net>.
- [27] I. S. Lim, H. Stoll, and P. Schwerdtfeger, *J. Chem. Phys.* **124**, 034107 (2006).
- [28] J. T. H. Dunning, *J. Chem. Phys.* **90**, 1007 (1989).
- [29] C. Hampel, K. Peterson, and H.-J. Werner, *Chem. Phys. Lett.* **190**, 1 (1992).
- [30] S. F. Boys and F. Bernardi, *Mol. Phys.* **19**, 553 (1970).
- [31] G. P. Yin, P. Li, and K. T. Tang, *J. Chem. Phys.* **132**, 074303 (2010).

- [32] A. Stein, H. Knöckel, and E. Tiemann, *Phys. Rev. A* **78**, 042508 (2008).
- [33] J. Yang, Y. Hao, J. Li, C. Zhou, and Y. Mo, *J. Chem. Phys.* **122**, 134308 (2005).
- [34] E. C. M. Chen and W. G. Wentworth, *J. Phys. Chem.* **89**, 4099 (1985).
- [35] F. Engelke, *Chem. Phys.* **39**, 279 (1979).
- [36] K.P. Huber and G. Herzberg, *Constants of Diatomic Molecules* (Van Nostrand Reinhold, New York, 1979).
- [37] W. E. Ernst, J. Kandler, S. Kindt, and T. Topping, *Chem. Phys. Lett.* **113**, 351 (1985).
- [38] S. R. Langhoff, J. C. W. Bauschlicher, and H. Partridge, *J. Chem. Phys.* **84**, 1687 (1986).
- [39] M. Kaupp, P. V. R. Schleyer, H. Stoll, and H. Preuss, *J. Am. Chem. Soc.* **113**, 6012 (1991).
- [40] J. M. W. Chase, *J. Phys. Chem. Ref. Data Monogr.* **9**, 1 (1998).
- [41] D. L. Hildenbrand, *J. Chem. Phys.* **48**, 3657 (1968).